Design of an Artificial Lung Compliance Chamber for Pulmonary Replacement

Jonathan W. Haft,* Joseph L. Bull,† Rebecca Rose,* Jeffrey Katsra,† James B. Grotberg,† Robert H. Bartlett,* and Ronald B. Hirschl*

Matching the impedance of an artificial lung for pulmonary replacement to native pulmonary impedance is important in preventing right ventricular dysfunction. A lumped-parameter theoretical model and bench-top experiments were used to investigate the effect of a prototype compliance chamber on input impedance. The bench-top simulation consisted of a pulsatile flow generator, a prototype compliance chamber, and a low resistance artificial lung connected in series. Effective compliance was varied using pneumatic compression. The theoretical model considered a similar circuit with resistors before and after a compliance element. The bundle flow pulsatility (flow amplitude divided by average flow) and input impedance were calculated in the theoretical and experimental models. More compliance and lower upstream resistance result in lower bundle flow pulsatility and reduced first harmonic impedance. Matching the time scale of the circuit to the period of pulsatile flow also reduces impedance. The bench-top circuit demonstrated an optimal chamber pressure at which first harmonic impedance is reduced by 80%. The prototype compliance chamber in series with the artificial lung more closely matches native pulmonary impedance. The lumped-parameter model and the bench-top simulation will aid in the design and testing of compliance chamber modifications to improve its efficiency. *ASAIO Journal* 2003; 49:35–40.

Lung transplantation is the only treatment for chronic end-stage respiratory failure. However, the shortage of donor organs limits its utility, as many potential recipients die while awaiting graft availability.[1] Various alternatives are currently under investigation to deal with this problem. Advances in gas exchange membrane technology have allowed the development of highly efficient oxygenators with low blood flow resistance.[2] A device constructed using these membranes can potentially serve as an artificial lung, with blood perfusion generated by the native cardiac output.

Total gas exchange support can be achieved with an artificial lung by diverting venous blood from the main pulmonary artery into the device, with return of oxygenated blood into the left atrium. With the distal pulmonary artery ligated, the entire cardiac output will bypass the pulmonary circulation, allowing the artificial lung to serve as a pulmonary replacement. This application is feasible only if the cardiac load generated by flow through the oxygenator is comparable with that of the native circulation.

Impedance is the opposition to pulsatile flow and defines cardiac load.[3] Unlike resistance, which is primarily dependent upon the length and cross-sectional area of the blood flow path, impedance is determined by the effect of compliance and pulse wave reflections produced by changes in blood path geometry. Impedance is typically expressed as a function of frequency or harmonic. Whereas zero harmonic impedance (Z_0) is equivalent to resistance, impedance at the integer harmonics represents the load to flow pulsations. In the pulmonary circulation, first harmonic impedance (Z_1) appears to be the most significant of these, as the majority of pulsatile flow exists within that harmonic.[4] Measurements of pulmonary input impedance in healthy human subjects have demonstrated Z_0 and Z_1 of approximately 1 and 0.5 Woods Units (mm Hg × min/L), respectively. We have found similar values in our comparably sized adult sheep animal model.[5]

Our laboratory has been testing a low resistance oxygenator, developed for use as an artificial lung.[5–7] We sought to design and test a compliance chamber that, when coupled in series with the artificial lung, matches pulmonary input impedance. Our investigation consisted of a bench-top simulation using a prototype design, guided by a theoretical lumped parameter model.

Methods

Lumped-Parameter Model

To understand how best to implement a compliance chamber with the artificial lung, we consider a three element lumped-parameter model (**Figure 1**). This circuit consists of a compliance element (C*) and two resistive elements (R_1* and R_2*) before and after the compliance element, respectively. The * indicates a dimensional value. The model was simplified by neglecting inertance and the specific velocity fields and other multidimensional fluid dynamical features of flow through the circuit. Lumped-parameter models with few elements have been shown to be effective in describing the human systemic circulation.[8]

The governing equation for a resistor is $\Delta P^* = R^* Q^*$, where ΔP^* and Q^* are the pressure drop flow and rate through the resistor. The governing equation for a compliance element is $Q^* = C^* dP^*/dt^*$, where t^* is time and P^* is the pressure across the compliance element. The equations were nondimensionalized using the characteristic scales of the problem:

From the *Department of Surgery, University of Michigan Health System; and the †Department of Biomedical Engineering, University of Michigan.

Submitted for consideration April 2002; accepted for publication August 2002.

Reprint requests: Dr. Ronald B. Hirschl, Department of Surgery, University of Michigan Health System, 1500 E. Medical Center Dr., Ann Arbor, MI 48109.

DOI: 10.1097/01.MAT.0000045714.41241.FF

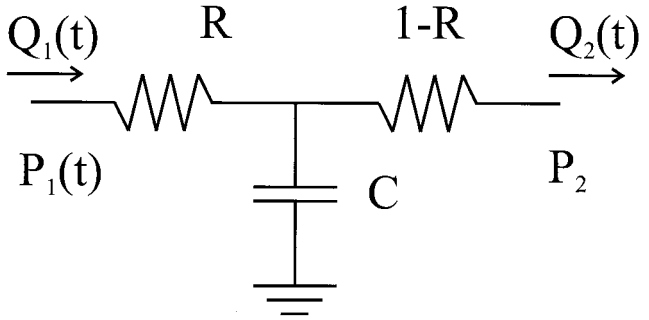

Figure 1. Three element lumped-parameter model. Resistance, compliance, and flow are nondimensionalized. For dimensional values, R and 1-R represent R_1* and R_2*, respectively.

$$P^* = (R^*_1 + R^*_2)Q_{\text{ref}}\, P \tag{1}$$

$$Q^* = Q_{\text{ref}}\, Q \tag{2}$$

$$R^*_i = (R^*_1 + R^*_2)\, R_i \tag{3}$$

$$t^* = T_{\text{pulse}} t \tag{4}$$

where T_{pulse} is the period of pulsatile flow, t is time, and Q_{ref} is the maximum value of the periodic inlet flow, Q_1*. Nondimensional variables are unstarred. The equations for all of the elements are then combined using continuity and the requirement that the total pressure drop along the circuit equal $P_1 - P_2$, where P_1 and P_2 are the nondimensionalized inlet and outlet pressures, respectively. This obtains the nondimensional governing equation of the system:

$$\frac{dP_1(t)}{dt} = -T\frac{P_1(t)}{1-R} + TQ_1(t)\left(1 + \frac{R}{1-R}\right) + R\frac{dQ_1(t)}{dt} \tag{5}$$

where the dimensionless parameters are defined as

$$T = T_{\text{pulse}}/(R^*_1 + R^*_2)C^* \tag{6}$$

$$R = R^*_1/(R^*_1 + R^*_2) \tag{7}$$

The outlet pressure (P_2) is assumed constant because left atrial pressure is nearly constant. T indicates the ratio of the time scale of the oscillatory flow to the natural time scale of the system, and R indicates the proportion of the total resistance that is proximal to the compliance chamber. The natural time scale of a resistor-compliance system is R^*C^* and indicates the time scale of exponential decay in flow if the system is filled and then allowed to empty because of elastic recoil in the absence of pumping, such that $Q(t^*) = Q_0^*\, e^{-t^*/R^*C}$, where Q_0* is the flow rate when initially allowed to leave the circuit. Using continuity, the exit flow rate is found to be

$$Q_2 = Q_1 - \frac{1}{T}\frac{dP_1}{dt} + \frac{R}{T}\frac{dQ_1}{dt} \tag{8}$$

To model the physiological situation, we specify Q_1 and P_2, cardiac output and left atrial pressure, respectively, based on data obtained from animal experiments. P_2 was kept constant to simulate unvarying left atrial pressure. The governing **equations 5 and 8** were solved for $P_1(t)$ and $Q_2(t)$, pulmonary artery pressure and flow through the pulmonary veins, respectively.

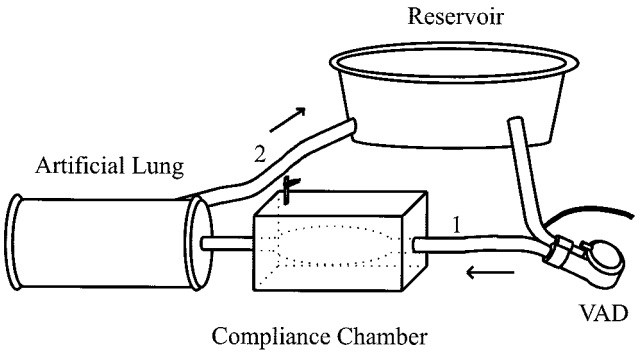

Figure 2. Schematic of the bench-top experiment. The VAD drives the flow through the compliance chamber and artificial lung into the reservoir. The reservoir provides a hydrostatic pressure, modeling the relatively constant pressure of the left atrium. VAD, ventricular assist device.

Two solution methods were used. The first was a fourth order Runge-Kutta numerical method. **Equation 5** was solved for $P_1(t)$ over one cycle, where $P_1(t)$ repeats for subsequent cycles. The time step was adjusted to obtain convergence, and $Q_2(t)$ was obtained over the entire cycle using **equation 8**. Second, an analytical method was used. The waveform $Q_1(t)$ was decomposed into a Fourier series, and an expansion for $P_1(t)$ was substituted into **equation 5**. The coefficients were solved at each order, using the orthogonality of the Fourier series, to determine $P_1(t)$. $Q_2(t)$ was then calculated from **equation 8** using the solution for P_1 (t). The results of the two methods agreed well.

The flow pulsatility of $Q_2(t)$ was calculated as the amplitude divided by the mean for several values of R at three different T values. The first harmonic of the input impedance spectra was calculated as $Z_1 = p_1/q_1$, where p_1 and q_1 are the amplitudes at the first harmonic of pressure and flow, respectively, which was obtained from the Fast Fourier Transformation of $P_1(t)$ and $Q_2(t)$.

Bench-Top Simulation

An experimental circuit was constructed consisting of a ventricular assist device (VAD) (Thoratec, Pleasanton, CA) to model pulsatile flow generated by the right ventricle (**Figure 2**). The VAD was pneumatically powered by a piston-driven respiratory pump (Harvard Apparatus Company, Dover, MA), at a fixed rate of 50 beats per minute. Flow was delivered to a prototype compliance chamber placed in series with an artificial lung (Michigan Critical Care Consultant, Ann Arbor, MI). The compliance chamber design incorporated a flaccid polyurethane bag externally compressed within a pneumatically pressurized airtight box (**Figure 3**). Outflow from the artificial lung was directed into an open air reservoir elevated to simulate a constant left atrial pressure of 10 mm Hg. Noncompliant polyvinyl chloride tubing (PVC) connected each of the elements.

Pressure was measured at the outlet of the VAD (P_1) and within the pressurized chamber (P_c) with a fluid coupled strain-gauge pressure transducer (Abbot Critical Care Systems, Chicago, IL), and the signals displayed continuously (Marquette Electronics, Milwaukee, WI). Flow was measured both at the outlet of the VAD (Q_1) and after the compliance chamber

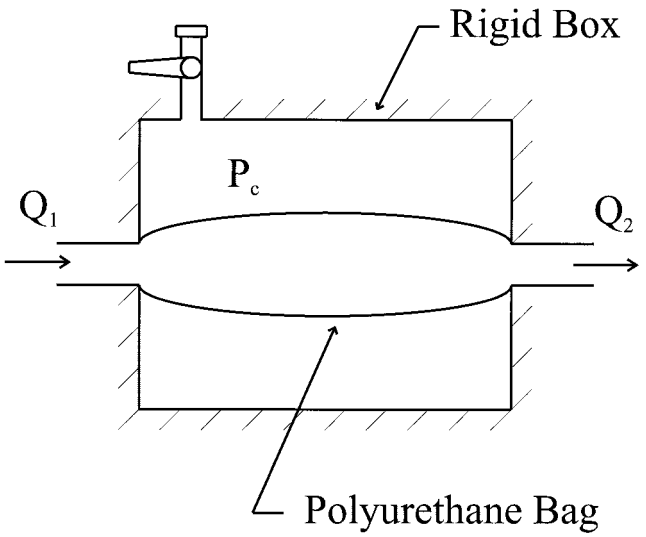

Figure 3. Sketch of compliance chamber. The pneumatic pressure inside the rigid box controls the compliance provided by the flaccid bag.

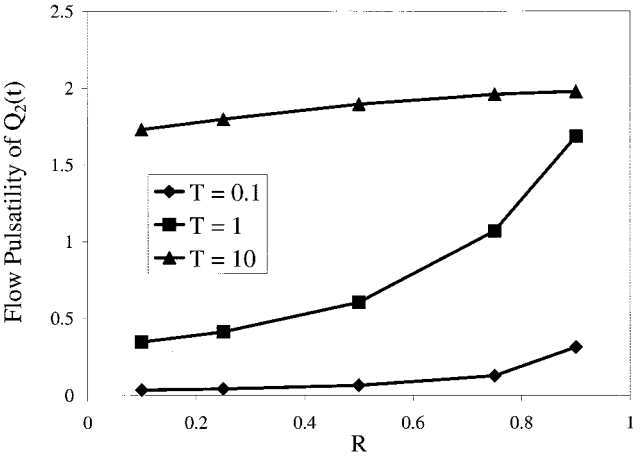

Figure 4. Flow pulsatility *vs.* R for T = 0.1, 1, and 10.

(Q_2) using a clamp-on ultrasonic flow probe (Transonic H13X6, Ithaca, NY), with mean values displayed on a flow meter (Transonic HT110). Data were collected at a sampling frequency of 300 Hz using a data acquisition system (National Instruments, Austin, TX) and stored on a personal computer (Apple Computers, Cupertino, CA). Using available software (Mathworks, Natick, MA), Fast Fourier Transformation was performed on P_1 and Q_1. Z_0 was determined by the ratio of mean pressure and flow, adjusted by subtracting the constant outlet pressure of 10 mm Hg. Z_1 was calculated by the ratio of the amplitudes of pressure and flow at the first harmonic. Bundle flow pulsatility (BFP) is the ratio of the amplitude of flow divided by the mean, calculated from Q_2.

The magnitude of external pneumatic compression within the chamber (P_c) was varied from 0 to 16 mm Hg. The size of the compliance chamber reservoir was also varied, using volumes of 50, 100, 250, and 500 ml. In addition, a 250 ml reservoir chamber was constructed with a stent to prevent complete chamber collapse with high levels of compression. The artificial lung was also tested in the absence of a compliance chamber (using noncompliant PVC tubing) as a control. Four acquisitions were made under each experimental condition, with data expressed as mean ± standard deviation. Statistical analysis was performed using analysis of variance with a post hoc Tukey test to account for multiple comparisons.

Results

Lumped-Parameter Model

The governing equation was solved for $Q_2(t)$ and $P_1(t)$, with $Q_1(t)$ specified based on data obtained from animal experiments and a constant P_2 to model the approximately constant left atrial pressure. The flow pulsatility of $Q_2(t)$ was calculated as the amplitude divided by the mean for several values of R at three different T values (**Figure 4**). The first harmonic of the input impedance spectra was calculated as $Z_1 = p_1/q_1$, where p_1 and q_1 are the amplitudes at the first harmonic of pressure and flow, respectively, obtained from the Fast Fourier Transformation of $P_1(t)$ and $Q_1(t)$. The zero and first harmonic impedances are shown in **Figure 5** for several values of R.

Bench-Top Simulation

Flow through the artificial lung in the absence of compliance generated Z_0 and Z_1 of 1.31 ± 0.01 and 4.61 ± 0.02 Woods Units, respectively. Addition of the compliance chamber without compression slightly increased resistance for all chamber volumes (1.63 ± 0.02, 1.55 ± 0.03, 1.67 ± 0.003, and 1.70 ± 0.10 for reservoir volumes of 50, 100, 250, and 500 ml, respectively; $p < 0.05$), but had no effect on Z_1.

External pneumatic compression of the compliance chamber reduced Z_1 for all chamber volumes, with the lowest Z_1 occurring while using the 250 ml reservoir compressed to 12 mm Hg (**Figure 6**). Compression beyond 12 mm Hg elevated Z_1. Pneumatic compression also reduced Z_0 at 12 mm Hg for all chamber volumes (**Figure 7**). Again, compression beyond 12 mm Hg resulted in Z_0 elevation. This effect was minimized with the use of the stented compliance reservoir. BFP was reduced with external pneumatic compression of the compli-

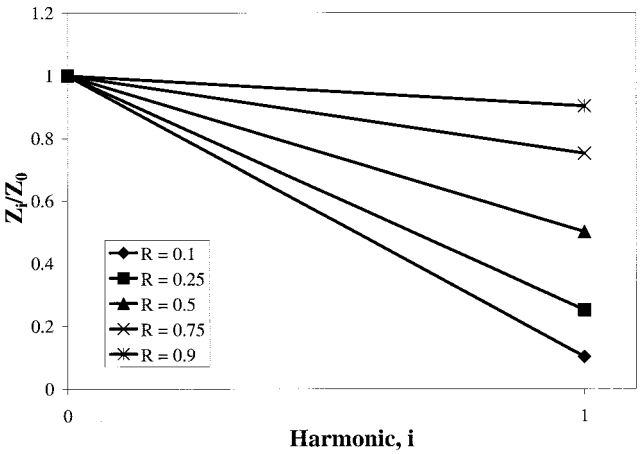

Figure 5. Zero and first harmonics of impedance for several values of R.

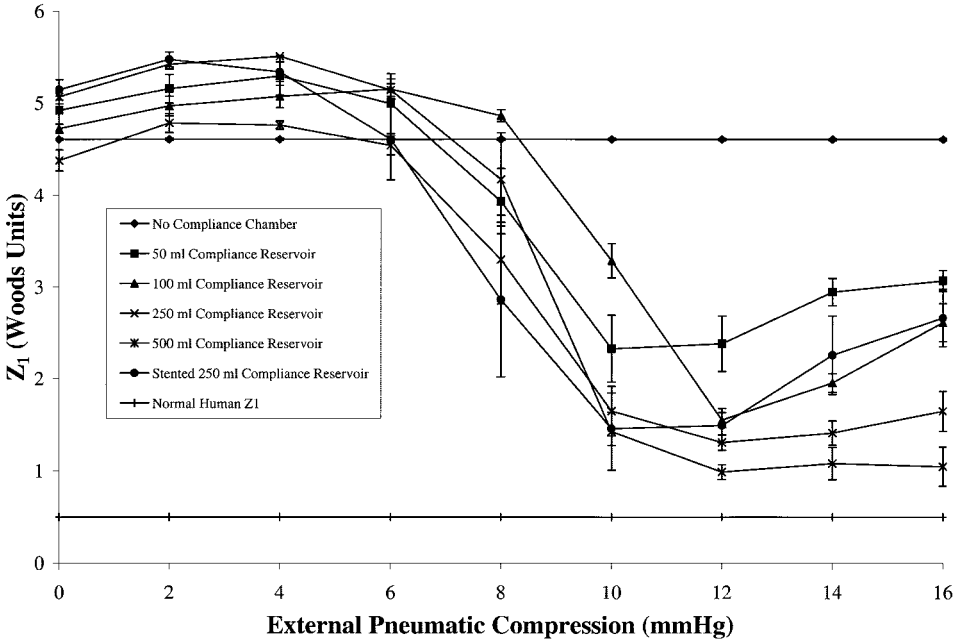

Figure 6. First harmonic impedance, Z_1, *vs.* external pneumatic compression for a variety of reservoir volumes. Data are expressed as mean ± standard error.

ance chamber. Minimum pulsatility was achieved with the 250 ml compliance reservoir when compressed at 14 mm Hg (**Figure 8**).

Discussion

Numerous laboratories are developing artificial lungs using a variety of designs and applications, all with the eventual goal of producing a viable bridge or alternative to lung transplantation. Extracorporeal life support (ECMO) has been successfully used as a short-term treatment of acute respiratory failure, serving as a bridge to recovery.[9] However, the practical duration of ECMO is limited by the complexity, cost, and inevitable complications that arise with prolonged treatment. In addition, ECMO in its current form can only be provided in the intensive care unit setting, with minute-to-minute direct observation by trained personnel. We believe that the complexity associated with ECMO can be attributed in large part to the mechanical pump required to generate blood flow and the necessary length of conduit tubing. An oxygenator with low resistance to blood flow can be perfused by the native cardiac output, thus obviating the need for a mechanical pump. This design allows for extracorporeal gas exchange but avoids the cellular blood element trauma associated with blood pumps

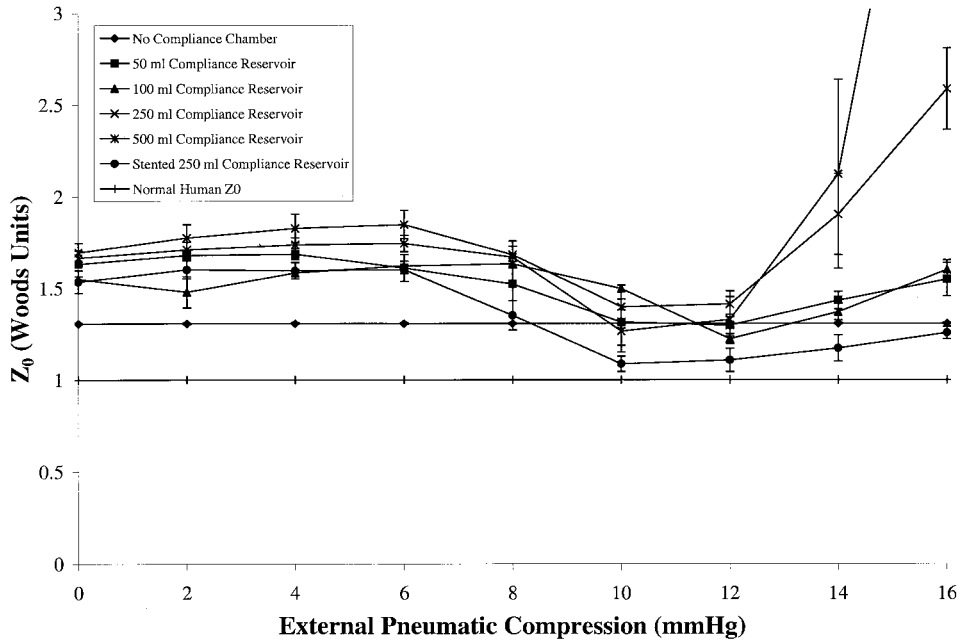

Figure 7. Resistance, Z_0, *vs.* external pneumatic compression for a variety of reservoir volumes. Data are expressed as mean ± standard error.

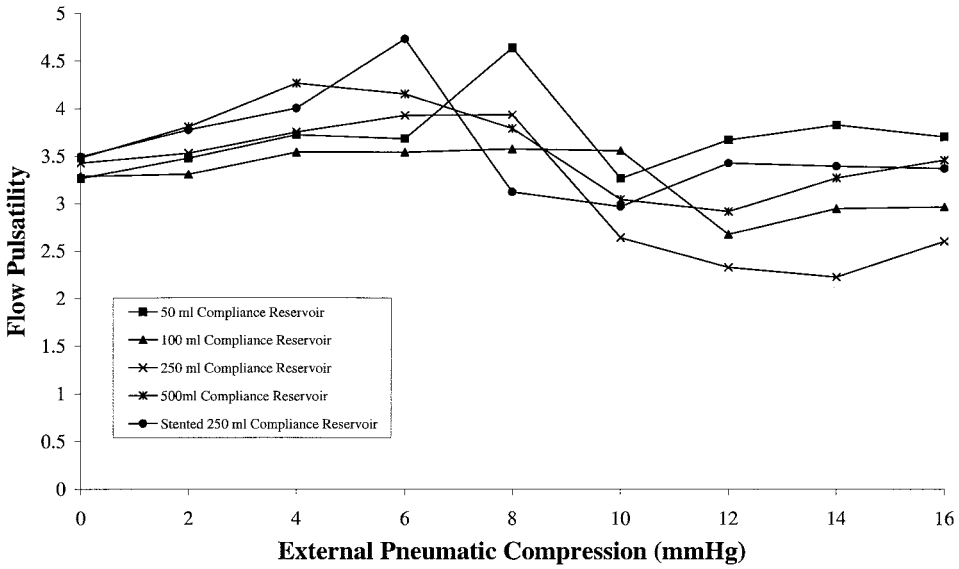

Figure 8. Bundle flow pulsatility *vs.* external pneumatic compression for a variety of reservoir volumes.

and potentially minimizes cost. In addition, the simplicity of this design appears practical for use as a long-term ambulatory treatment.

Several potential applications can be used incorporating venous delivery through an artificial lung. A theoretical lumped-parameter model has previously described the impact in terms of cardiac load for several of these approaches.[10] When the inflow blood from the right ventricle is returned into the left atrium, flow can either be exclusively through the artificial lung, as in pulmonary replacement, or competitive with the native pulmonary circulation, providing partial respiratory support. The parallel support approach will not increase right ventricular load, as the compliance of the pulmonary vascular bed will remain in place. In fact, this application can significantly reduce cardiac load in the setting of severe pulmonary hypertension and right ventricular failure, as is frequently present in patients with end-stage lung disease.[5] However, this application cannot satisfy all of the gas exchange requirements as some pulmonary blood flow continues, potentially leaving some patients hypoxic. In addition, patients such as those with cystic fibrosis may be at greater risk of infectious complications by leaving the pyogenic native lungs in place. Total support in the form of artificial pulmonary replacement may be more appropriate in these cases. However, as demonstrated in the previous lumped-parameter model, this configuration can drastically alter cardiac load, potentially resulting in right ventricular failure.

The bench-top simulation used in this study is a simplified model of the right-sided circulation, with a VAD producing physiologic pulsatile flow and an elevated reservoir generating a hydrostatic pressure to reproduce relatively constant left atrial pressure. Several limitations in this bench-top system can be elucidated, such as the fixed pump rate, stroke volume, and the use of water in the system rather than blood. Further studies accounting for these limitations are undoubtedly necessary. However, the ease of preparation and its reproducibility make this simulation a satisfactory initial assessment of the cardiac load produced by an artificial lung with a prototype compliance chamber.

The resistance of the artificial lung used in this study is comparable with the resistance of the native pulmonary vascular bed of normal patients. However, when exposed to pulsatile flow, the lack of compliance and the presence of abnormal pulse wave reflections result in an impedance at the first harmonic nearly 10-fold higher than that seen in normal lungs. The consequences of elevated input impedance on cardiac function *in vivo* have not been described. A previous study using isolated hearts in a modified extracorporeal circuit demonstrated abnormal ventricular function with reductions in outflow compliance and elevations in impedance.[11] Addition of a compliance chamber that reduces impedance may prevent these abnormalities.

The results of the lumped-parameter model are useful in interpreting the bench-top simulation and can provide guidance in constructing a compliance chamber. Two main considerations for this design are reducing the flow pulsatility across the artificial lung membrane and decreasing first harmonic impedance. Because higher harmonics of flow and pressure are relatively small, the first harmonic provides a good indication of how closely the artificial and native circulations match.

As shown in **Figure 4**, values of T in the range of one and smaller decrease fiber BFP. Matching the time scale of flow pulsations with the time scale of the resistance-compliance circuit allows the compliance chamber volume to increase during ejection and then decrease before the next cycle. If the time scale of the circuit is significantly faster than the period of pulsations, the reservoir quickly returns stored volume. Outflow becomes similar to inflow, minimizing the effectiveness of compliance. Lowering R reduces first harmonic impedance, indicating that having most of the circuit resistance distal to the compliance chamber optimizes its efficiency. Additionally, BFP is also lower when R is small, demonstrating the relationship between first harmonic impedance and BFP. A more efficient compliance chamber design will dampen flow pulsations and reduce impedance at the first harmonic. From the lumped-parameter model, a compliance chamber design should be such that the time scale of the circuit is matched to

the time scale of the flow and that most of the circuit resistance is positioned after the compliance element.

The prototype compliance chamber design used in this study reduced first harmonic impedance from 4.6 to 1.0 Woods Units, without increasing steady flow resistance (**Figures 6 and 7**). This nearly 80% reduction is a significant improvement in pulsatile load, although we were not quite able to achieve the 0.5 Woods Units Z_1 typically seen in normal patients. Based on the lumped-parameter model, one reason for the inability achieving the desired Z_1 is possibly related to the increased Z_0 observed at higher pneumatic pressures (**Figure 7**). In the terminology of the lumped-parameter model, C may have been increased, but R was also increased, preventing additional reductions in Z_1. Further studies using analytical techniques such as computational fluid dynamics will address many of the design limitations, and potentially allow prototype refinement to more closely approximate normal pulmonary input impedance.

External compression maximizes compliance and alters its time scale by augmenting diastolic emptying and maximizing its capacitance before the initiation of systole. However, compression of a deformable material will reduce the cross-sectional area of the blood flow path, potentially increasing steady flow resistance. In our simulation, once compression exceeded the hydrostatic forces of the "left atrium," there was a consistent rise in Z_0, markedly so in several cases (**Figure 7**). This drawback could be avoided, however, with the use of the stented compliance reservoir, preventing its complete collapse.

A compliance chamber intended for prolonged use with an artificial lung must adhere to some basic guidelines: durability, biocompatibility, and adjustability. Once subjected to repeated stress cycles, elastic materials with known biocompatibility will develop fatigue and eventual failure. This loss of compliance will inevitably elevate impedance and potentially result in right ventricular failure. Loss of elasticity may also produce stagnation and promote thrombosis, an equally catastrophic consequence. Using pneumatic compression on a deformable but nonelastic material, fatigue can be avoided. Additionally, air pressure can be continuously monitored and adjusted. In our experimental simulation, optimal impedance was achieved when compression slightly exceeded "left atrial" hydrostatic pressure. As physiologic conditions change, such as alterations in left atrial pressure, heart rate, or stroke volume, external compression can be modified to maintain the necessary compliance and adjust its time scale, thus compensating to minimize cardiac load. Servoregulation can also be incorporated to provide smooth automation.

Conclusion

This study tested a design for an artificial lung compliance chamber, guided by a theoretical three element lumped-parameter model. The low resistance but noncompliant artificial lung demonstrated similar resistance but significantly higher impedance when compared with the normal pulmonary circulation. Addition of an in-series compliance chamber significantly reduced first harmonic impedance, without increasing resistance. The design incorporates a deformable biocompatible material, optimally compliant independent of its mechanical elasticity. Further refinements using analytic tools and bench-top simulation should allow the development of a design that closely reproduces normal pulmonary input impedance in a practical and functional package. Correlation with *in vivo* testing will be performed to evaluate the effect of compliance on right ventricular function.

References

1. Arcasoy SM, Kotloff RM: Medical progress: Lung transplantation. *N Engl J Med* 340: 1081–1091, 1999.
2. Zwischenberger JB, Anderson CM, Cook KE, Lick SD, Mockros LF, Bartlett RH: Development of an implantable artificial lung: Challenges and progress. *ASAIO J* 47: 316–320, 2001.
3. Milnor WR: Pulsatile blood flow. *N Engl J Med* 287: 27–34, 1972.
4. Kussmaul WG, Altschuler JA, Matthai WH, Laskey WK: Heart failure: Right ventricular-vascular interaction in congestive heart failure: Importance of low frequency impedance. *Circulation* 88: 1010–1015, 1993.
5. Haft JW, Montoya JP, Alnajjar O, *et al:* An artificial lung reduces pulmonary input impedance and improves right ventricular efficiency in acute pulmonary hypertension. *J Thorac Cardiovasc Surg* 122: 1094–1100, 2001.
6. Fazzalari FL, Montoya PJ, Bonnell MR, Bliss DW, Hirschl RB, Bartlett RH: The development of an implantable artificial lung. *ASAIO J* 40: M728–731, 1994.
7. Lynch WR, Montoya PJ, Brandt DO, Schreiner RJ, Iannettoni MD, Bartlett RH: Hemodynamic effect of a low resistance artificial lung in series with the native lungs of sheep. *Ann Thor Surg* 69: 351–356, 2000.
8. Sharp MK, Dharmalingam RK: Development of a hydraulic model of the human systemic circulation. *ASAIO J* 45: 535–540, 1999.
9. Kolla S, Awad SS, Rich PB, Schreiner RJ, Hirschl RB, Bartlett RH: Extracorporeal life support for 100 adult patients with severe respiratory failure. *Ann Surg* 226: 544–564, 1997.
10. Boschetti F, Perlman CE, Cook KE, Mockros LF: Hemodynamic effects of attachment modes and device design of a thoracic artificial lung. *ASAIO J* 46: 42–48, 2000.
11. Piene H, Sund T: Flow and power output of right ventricle facing load with variable input impedance. *Am J Physiol* 237: H125–H130, 1979.